

# Osteoblast proliferation and maturation on bioactive fiber-reinforced composite surface

Ahmed Mansour Ballo · Anne K. Kokkari · Ville V. Meretoja ·  
Lippo L. Lassila · Pekka K. Vallittu · Timo O. Narhi

Received: 12 February 2007 / Accepted: 8 April 2008 / Published online: 25 April 2008  
© Springer Science+Business Media, LLC 2008

**Abstract** The objective of this study was to evaluate the proliferation and osteogenic potential of bone-marrow derived osteoblast-like cells on fiber-reinforced composite (FRC) substrates with and without bioactive glass surface modification. Three FRC materials were fabricated for the study: (a) grit-blasted FRC, (b) grit-blasted FRC with bidirectional net reinforcement and (c) FRC with bioactive glass (BAG) coating. Rat bone-marrow derived osteoblast-like cells were harvested and cultured on experimental material plates and on cp. titanium plates (control) for 21 days. The materials' surfaces were characterized by roughness testing and scanning electron microscopy. Cell growth and differentiation kinetics were subsequently investigated by evaluating proliferation, alkaline phosphatase (ALP) activity, osteocalcin (OC) and bone sialoprotein (BSP) production. On day 14, the cell proliferation was significantly lower ( $P < 0.05$ ) on FRC-BAG than on titanium and FRC. The proliferation on the other three materials was equal throughout the experiment. The maximal ALP activities on FRC, FRC-Net, and titanium were observed on day 21, whereas FRC-BAG had already reached the maximal level on day 14. Expression of osteoblastic markers (OC, BSP) indicates that the fastest osteogenic differentiation takes place on FRC after 7 days. In contrast, a slower differentiation process was observed on titanium than on any other tested material ( $P < 0.015$ ) at 21 days, as was confirmed by increased mRNA expression of OC and BSP. It can be concluded that the

proliferation and maturation of osteoblast-like cells on FRC appears to be comparable to titanium. Presence of BAG enhances cell maturation.

## 1 Introduction

Commercially pure titanium and titanium alloys are traditional materials used in most commercially available endosseous implants. The success of an oral implant is primarily based on good osseointegration, which depends on the biocompatibility of the implant material and implant surface properties, as well as on bone quantity and quality [1, 2]. New bone formation at the implant–bone interface is a complex process. During the initial few seconds after implantation, extracellular matrix proteins occupy the implant surface which then aid osteoprogenitor cell attachment. This phenomenon in the early stage of healing is believed to be fundamental for the final osseointegration process [3].

Several osteoblast cell culture studies have been performed to investigate the biocompatibility of titanium implant surfaces [4, 5]. Those studies have shown that surface topography and composition have a strong influence on osteoblast differentiation. A rough titanium surface has shown to enhance the osteogenic potential of osteoblast-like cells when compared to that on a smooth titanium surface [6]. Chemical modification of implant surfaces has been found to improve bone apposition during early stages of bone regeneration [7], which then enhances osteoconduction on the implant surface [8]. An implant device fabricated totally from a solid titanium metal cannot always satisfy the requirements for optimal function and biologic behavior. Therefore, implants and prostheses that combine

---

A. M. Ballo (✉) · A. K. Kokkari · V. V. Meretoja ·  
L. L. Lassila · P. K. Vallittu · T. O. Narhi  
Department of Prosthetic Dentistry and Biomaterials Science,  
Institute of Dentistry, University of Turku,  
Lemminkäisenkatu 2, Turku 20520, Finland  
e-mail: ahmbal@utu.fi

different materials in coatings, or consist of composite materials, can offer more alternatives for various clinical situations.

Fiber-reinforced composites (FRCs) are durable materials with lower elastic modulus than metals [9]. In fact, the mechanical properties and modulus of elasticity of unidirectional FRC (20–40 GPa) are close to those of natural bone [10]. There is growing interest in using FRCs in dental applications and surgical implants for orthopedic and head and neck surgery involving some degree of structural performance under load-bearing conditions [11–15], which makes FRCs interesting materials also in load-bearing bone-anchored devices. Our previous studies concerning the mechanical properties of a FRC device designed for bone implantation have shown adequate performance in a laboratory environment [16]. However, for an implant material to be successful in a clinical setting it has to facilitate osteoblast attachment and new bone formation.

Several synthetic materials have been evaluated for implant coatings [17, 18]. However, fibrous tissue formation between the implant and bone has been a frequent complication, while direct bone bonding to implant surface is restricted to calcium phosphate ceramic materials [19–21]. Bioactive glasses (BAG) are one group of materials applied for this purpose [22]. BAG bonds to living bone through the formation of a hydroxyl carbonate apatite layer on their surface [23]. Furthermore, the dissolution products of the BAG can promote proliferation and differentiation of osteogenic cells [24, 25]. BAG provides a favorable environment for human osteoblast proliferation and function [26–28]. BAG implant coatings have been shown to improve osseointegration in both in vitro and in vivo conditions [29, 30]. BAG particles may be used as a bioactive component in FRC devices since they can be embedded within the resin matrix or applied to the surface of the FRC implants.

The aim of this study was to evaluate the proliferation and osteogenic potential of bone-marrow derived osteoblast-like cells on FRC substrates. The study is based on the working hypothesis that addition of BAG particles to the FRC surface promotes osteoblast behavior on the FRC.

## 2 Materials and methods

### 2.1 Preparation of the specimens

The materials used to fabricate the different specimens are listed in Table 1. Reinforcing continuous unidirectional E-glass fibers (composition: 55% SiO<sub>2</sub>, 15% Al<sub>2</sub>O<sub>3</sub>, 22% CaO, 6% B<sub>2</sub>O<sub>3</sub> and 0.5% MgO, >1.0% Fe + Na + K) were manually impregnated in a light curing bisGMA-TEGDMA resin for 24 h. Five bundles of fibers were incorporated in a mold to manufacture 1 mm-thick FRC plates (FRC group). For the second group (FRC Net group), porous PMMA/E-glass weave (Stick Net, Stick Tech, Turku, Finland) was preimpregnated for 24 h in light curing resin (Stick Resin Stick Tech, Turku, Finland) to dissolve the PMMA and to form a semi-IPN polymer network. The glass fiber weave was subsequently pressed on the FRC plate.

For the third group, the FRC plates were immersed in distilled water for 3 days to leach any residual monomers followed by heat drying, after which a mixture of bioactive glass particles and light curing Stick resin (2 g/ml) was prepared and applied only to the surface of the specimens (FRC-BAG group).

FRC plates were then polymerized in a light-curing oven (Visio Beta Vario 3 M/ESPE, Seefeld, Germany) at 60°C in a vacuum for 15 min to eliminate the oxygen inhibition layer on the FRC. The polymerization was subsequently completed in a light-curing oven (LicuLite, Dentsply De

**Table 1** Materials used in the study

Composition	Lot no.	Manufacture	Description	Product
BisGMA- <sup>a</sup> TEGDMA <sup>b</sup>	54031672	Stick Tech, Turku, Finland	Light curing resin	Stick Resin
E-glass <sup>c</sup> PMMA <sup>d</sup>	2050523-W 0053	Stick Tech, Turku, Finland	Polymer preimpregnated bidirectional weave fiber	Stick net fiber
E-glass	11372313	Ahlstrom, Karhula, Finland	Unidirectional fiber	E-glass fiber
BAG <sup>e</sup> SiO <sub>2</sub> 53%, Na <sub>2</sub> O 23%, CaO 20% and P <sub>2</sub> O <sub>5</sub> 4%	ABM S53-8-01	Vivoxid Ltd, Turku, Finland	Average particle size, 45 μm	BAG granule

<sup>a</sup> Bis-GMA, bisphenol A-glycidyl dimethacrylate

<sup>b</sup> TEGDMA, triethyleneglycol-dimethacrylate

<sup>c</sup> E-glass, electrical glass

<sup>d</sup> PMMA, polymethyl-methacrylate

<sup>e</sup> BAG, Bioactive Glass

Trey GmbH, Dreieich, Germany) for 1 h, during which the temperature was increased to 80°C (Kerr-Have., I, USA). To optimize the degree of monomer conversion (DC%), the specimens were post-cured in an oven for 24 h at 120°C, which is close to the glass transition temperature ( $T_g$ ) of pBisGMA-pTEGDMA-copolymer. Finally, all FRC plates except the one with BAG coating were immersed in distilled water for 3 days (37°C) to leach residual monomers.

In this study the experimental FRC plates and (control group) titanium plates (grade II) were grit-blasted with Al<sub>2</sub>O<sub>3</sub> particles (size 50–60 μm; Danville Engineering, USA). After surface preparation, square-shaped 10 × 10 × 1 mm specimens were cut out from the plates and the specimens were cleaned ultrasonically for 20 min in distilled water. The surface roughness of experimental FRC plates and titanium plates (control group) were measured (Surface roughness tester, Mitutoyo 301, Kawasaki, Japan).

The specimens, classified into the four following groups, were sterilized by autoclaving at 120°C for 20 min:

- (I) Blasted FRC (FRC group).
- (II) Blasted FRC with bidirectional fiber weave on the surface (FRC-Net group).
- (III) Blasted FRC with BAG coating (FRC-BAG group).
- (IV) Blasted commercially pure (grade 2) titanium (cpTi) (control group).

## 2.2 Cell cultures

Rat bone marrow stromal cells were harvested and cultured according to Maniopoulos et al. [31]. Briefly, femurs were isolated from two 6-week-old male Sprague–Dawley rats. The bones were wiped with 70% alcohol and immersed twice in α-MEM (Sigma chemical Co., USA) culture medium containing 100 units/ml of penicillin/streptomycin (Gibco BRL, Life Technologies BV, The Netherlands). The condyles were cut off, and the bone marrow was flushed out using complete cell culture medium (α-MEM) with 15% fetal bovine serum (Gibco) and supplemented with 50 μg/ml ascorbic acid (Sigma), 7 mM Na-β-glycerophosphate (Merck, Germany), and 10 nM dexamethasone (Sigma). The resulting suspension was passed through a 22-gauge needle. The adherent cell population was cultured in a humidified 5% CO<sub>2</sub> atmosphere at 37°C.

After 7 days of primary culture, cells were trypsinized and resuspended in complete culture medium. Cell culture substrates were placed into non-treated 24-well plates (Corning, USA) and washed with phosphate-buffered saline (PBS) for 1-h and with complete cell culture medium for 3 h at 37°C. Cell suspension was subsequently added to the test substrates at a density of 20,000 cells/cm<sup>2</sup> and

allowed to adhere overnight. After seeding, osteoblast culture was continued for three weeks with medium replacement every 2–3 days.

Cells seeded on conventional tissue culture polystyrene wells at a density of 10,000 cells/cm<sup>2</sup> were used as a positive cell control. The cells expanded to confluence, and exhibited typical osteogenic phenotype, starting to mineralize after 14 days of culture.

## 2.3 Ion concentration analysis

Silica and calcium concentrations in the used cell culture medium were analyzed from four to six replicate culture wells before each medium change. Three parallel measurements were carried out from each medium sample.

Colorimetric measurement of silica concentration was based on the molybdenum blue method [32]. The silico-molybdate complex was reduced with a mixture of 1-amino-2-naphthol-4-sulphonic acid and sulphite, and tartaric acid was used to eliminate interference from phosphate. Calcium concentrations were determined using the ortho-cresolphthalein complexone (OCPC) method [33]. The assay reagent consisted of OCPC with 8-hydroxyquinol in an ethanolamine/boric acid buffer. Absorbances (820 nm for silica and 560 nm for calcium) were measured using either a UV-1601 spectrophotometer (Shimadzu, Australia) or a Multiskan MS ELISA plate reader (Labsystems, Finland).

## 2.4 Proliferation assay

The amounts of cultured cells were determined using AlamarBlue™ (AB) assay (BioSource International, USA) in colorimetric format. At predetermined times, specimens ( $n = 4$ ) were withdrawn from the culture, and placed into clean 24-wells. Fresh assay solution (phenol red-free DMEM with 10% serum and including 10% AB reagent) was added to the wells. After 3 h incubation, absorbance values of the solution were taken at 560 nm and 595 nm using the ELISA plate reader. The measured absorbances were used to calculate the reduction of AB reagent in accordance with the manufacturer's instructions. Reductive cell activity of cultured osteoblasts has been shown to correlate with their numbers [34]. The cell activities were normalized in relation to the activity of the titanium control at the first time point.

## 2.5 Alkaline phosphatase activity

At predetermined times, four replicate specimens were washed with phosphate-buffered saline (PBS) and placed into clean 24-well containing 750 μl lysis buffer (25 mM HEPES, 0.1% Triton X-100, 0.9% NaCl, pH 7.6).

Immersed specimens were stored at  $-70^{\circ}\text{C}$  until the amounts of total protein and alkaline phosphatase (ALP) activity were measured from supernatants diluted with 0.9% NaCl as needed.

Amounts of total protein were measured with a Micro BCA<sup>TM</sup> protein assay reagent kit (Pierce, USA) according to the manufacture's microwell plate protocol. Briefly, equal amounts of supernatant and working reagent were combined and incubated at  $37^{\circ}\text{C}$  for 2 h. Mean readings of absorbances from three replicate wells were recorded at 560 nm, using the ELISA plate reader. Protein concentrations were read from a bovine albumin (Pierce) standard curve.

To measure ALP activity, 50  $\mu\text{l}$  of supernatant and 200  $\mu\text{l}$  of para-nitrophenyl phosphate substrate solution (Sigma) were combined on a microwell plate. The plate was incubated at  $37^{\circ}\text{C}$  for 1 h and 50  $\mu\text{l}$  of 3 M NaOH solution was added to each well to stop the enzymatic reaction. Mean readings of absorbance from three replicate wells were recorded at 405 nm, using the ELISA plate reader. Amounts of converted substrate were read from a para-nitrophenol standard curve. Measured ALP activities were normalized in relation to the amounts of protein determined.

## 2.6 RT-PCR

At predetermined times, total cellular RNA from culture substrates was isolated using Trizol<sup>®</sup> reagent (Gibco). Four replicates from each substrate type were reverse transcribed with random hexamer primers using a GeneAmp Gold RNA PCR Reagent kit (Applied Biosystems, USA). The resultant first-strand cDNA was analyzed in duplicate PCR reactions using FAM-labeled TaqMan<sup>®</sup> Gene Expression Assays (Applied Biosystems) for bone sialoprotein (BSP; Rn00561414\_m1), osteocalcin (OC; Rn00566386\_g1) and glyceraldehyde-3-phosphate dehydrogenase (GAPDH, a control gene; Rn99999916\_s1). PCRs were carried out using an iCycler iQ real-time PCR detection system with software version 3.1 (Bio-Rad Laboratories). The following cycling conditions were used:  $95^{\circ}\text{C}/5$  min; 40 cycles of  $95^{\circ}\text{C}/20$  s,  $60^{\circ}\text{C}/60$  s. The threshold cycles ( $C_T$ ) were automatically calculated using "the maximum curvature approach" and gene expression levels of BSP and OC were normalized to GAPDH expression in each RNA sample ( $\Delta C_T = C_{T, \text{target}} - C_{T, \text{GAPDH}}$ ). A difference of one unit in  $\Delta C_T$  value corresponds to a two-fold difference in gene expression level.

## 2.7 Scanning electron microscopy and histological staining

Scanning electron microscopy (SEM) and histological examination after staining were used to visualize the

progression of osteoblast cultures. Cell culture substrates were washed in PBS and fixed with 2% glutardialdehyde in a 100 mM cacodylic acid buffer (pH 7.4). The fixed specimens were rinsed in buffer and either dried in a rising alcohol series or stored in 70% ethanol for a subsequent SEM analysis and histological staining, respectively.

Dried specimens for SEM were carbon-coated before imaging (JSM-5500; JEOL Ltd., Japan). Histological specimens were re-hydrated in distilled water, stained with Weigert–van Gieson and dried in a rising alcohol series. The specimens were observed under a stereo microscope and photographed with a digital camera.

## 2.8 Statistical analysis

Statistical analysis was performed with an SPSS v.11.0 software package (SPSS Inc., USA). Data were analyzed with one-way ANOVA followed by Tukey's post-hoc test.

# 3 Results

## 3.1 Specimens' surfaces characteristic

The blasting produced an overall Ra of  $1.97 \pm 0.26$   $\mu\text{m}$  for the FRC group,  $4.90 \pm 0.30$   $\mu\text{m}$  for the FRC-Net group,  $3.28 \pm 0.22$   $\mu\text{m}$  for the FRC-BAG group and  $0.97 \pm 0.10$   $\mu\text{m}$  for the titanium group. Scanning Electron Micrograph (SEM) analysis of the surface morphology showed a rough surface with a large variety of appearing structures among the different FRC groups (Fig. 1; SEM panel after 1 day of culture).

## 3.2 Cell proliferation

The proliferation of osteoblasts on different surfaces was measured over a period of 21 days. The cell activity on all the tested materials increased with time. Within the first week of culture there were no significant differences in proliferation, as indicated by the Alamar Blue assay (Fig. 2). On day 14, however, the cell activity on FRC-BAG was significantly lower ( $P < 0.05$ ) than on titanium and FRC. The cell activity on FRC-BAG also remained lower on day 21, albeit with no significant difference. The proliferation on the other three materials was equal throughout the experiment.

Histological staining (Fig. 3) and SEM micrographs (Fig. 4; SEM panel after 14 days of culture) showed good cell proliferation and spreading over the material surfaces. A semi-confluent cell layer was formed by day 7, whereas a multilayer of cells with a collagen-rich matrix entirely

**Fig. 1** Scanning electron micrograph of the surface morphology showed a rough surface with a large variety of appearing structures among the different FRC groups. (a) FRC, (b) FRC-BAG, (c) FRC-net, (d) Titanium

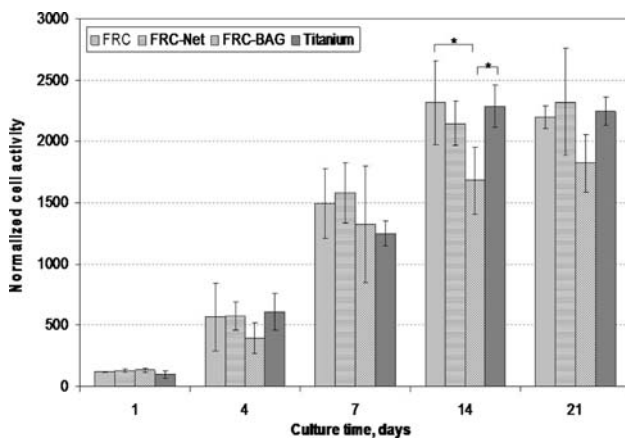
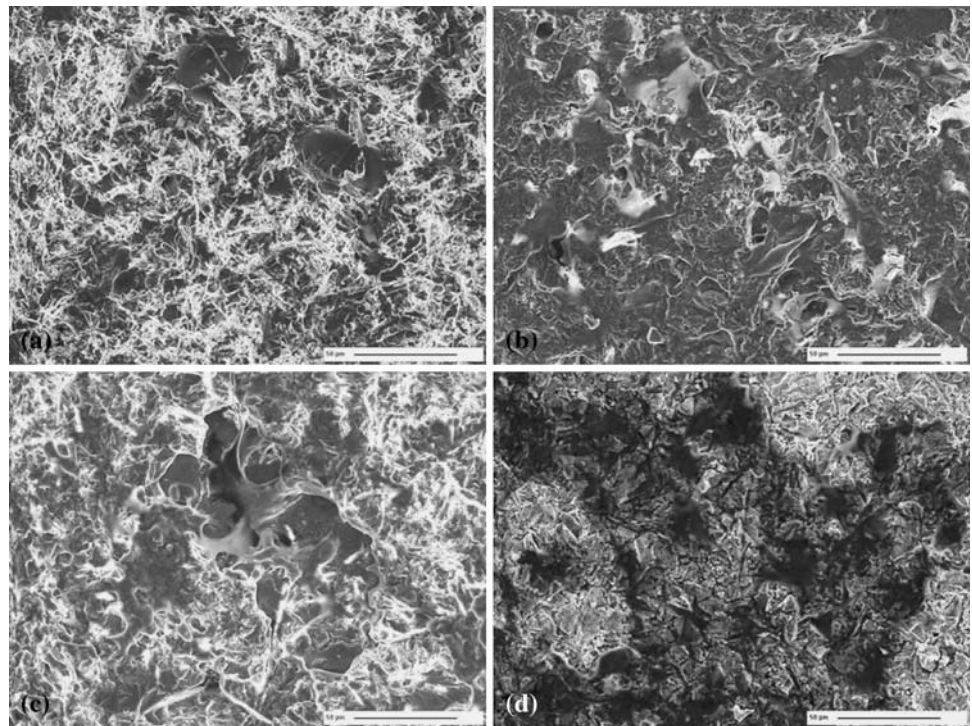


**Fig. 2** Cell proliferation with cultured substrates after 1, 4, 7, 14 and 21 days. Error bars represent standard deviations and \* indicates a statistically significant difference ( $P < 0.05$ ) between materials

covered all the substrate types by day 14. No differences among the materials were observed.

### 3.3 Alkaline phosphatase activity

Alkaline phosphatase (ALP) activity was measured after 4, 7, 14, and 21 days of culture, and it increased with time (Fig. 5). The maximal ALP activities on FRC, FRC-Net, and titanium were observed on day 21. FRC-BAG had already reached the maximal level on day 14, and on day 21 the activity was significantly lower than on the other materials ( $P < 0.05$ ).

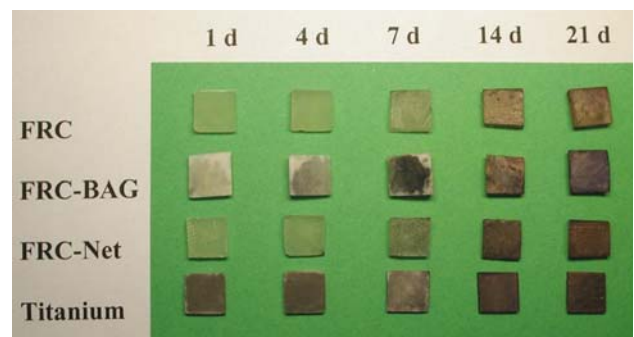


**Fig. 3** Digital picture of Weigert–van Gieson stained cell culture substrates. Proliferation can be noticed as increasing color intensities by time. On day 14, multilayer of cells cover the whole substrate area

### 3.4 Ion concentration analysis

Dissolution of BAG from FRC-BAG specimens released alkali ions and soluble silica into the cell culture medium. Leached alkali increased culture pH by 0.1–0.2 units when compared to other materials (data not shown). Furthermore, high concentrations of calcium and silica were initially observed (Fig. 6). The ion concentrations with FRC-BAG substrates started to decline by day 9, likely indicating the onset of mineralization. Cells on FRC-BAG substrates started to mineralize by day 9, as indicated by depletion of calcium from the culture medium. Calcium concentrations in the used culture mediums were significantly lower ( $P < 0.05$ ) than those in medium blanks from day 9 onwards. However, on days 9 and 11 there was

**Fig. 4** Scanning electron micrograph of osteoblast-like cells after 14 days of culture. (a) FRC, (b) FRC-BAG, (c) FRC-net, (d) Titanium

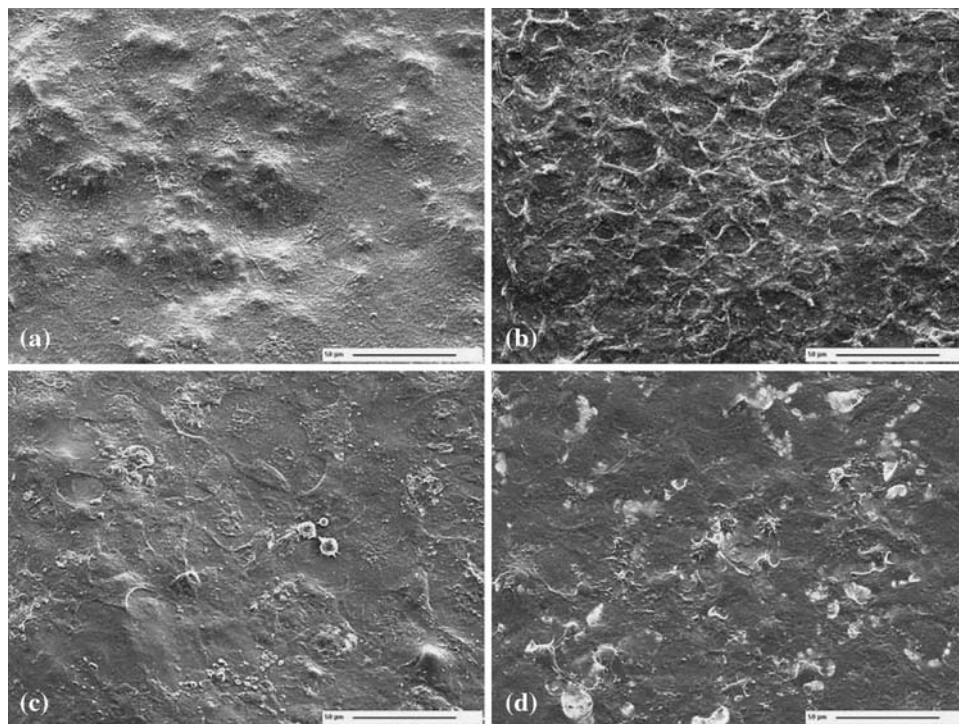
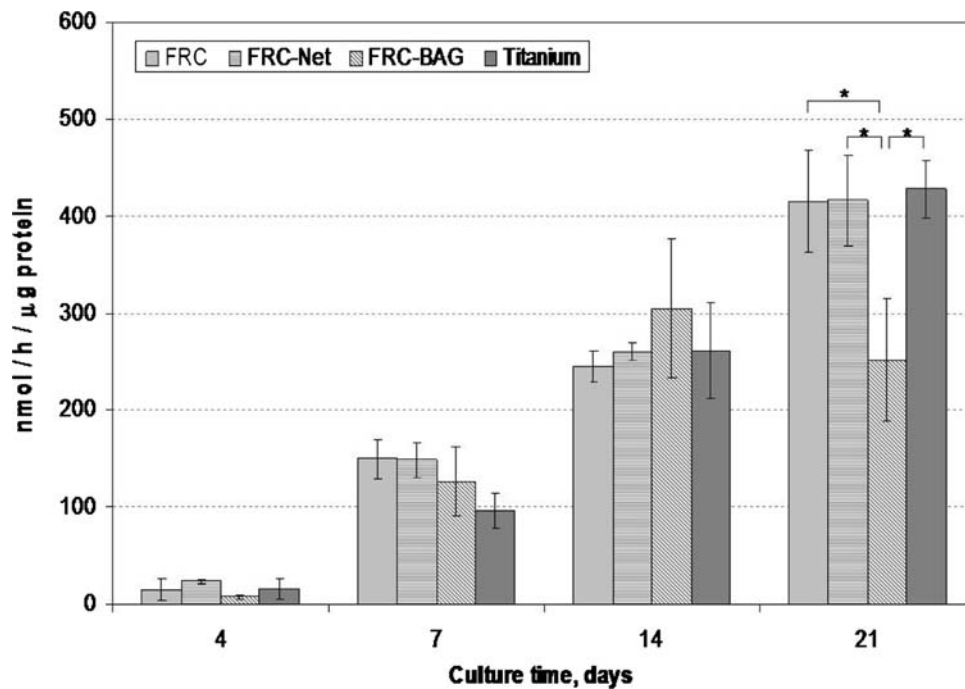


**Fig. 5** The evolution of ALP activities during 3 weeks culture. Error bars represent standard deviations and \* indicates a statistically significant difference ( $P < 0.05$ ) between materials



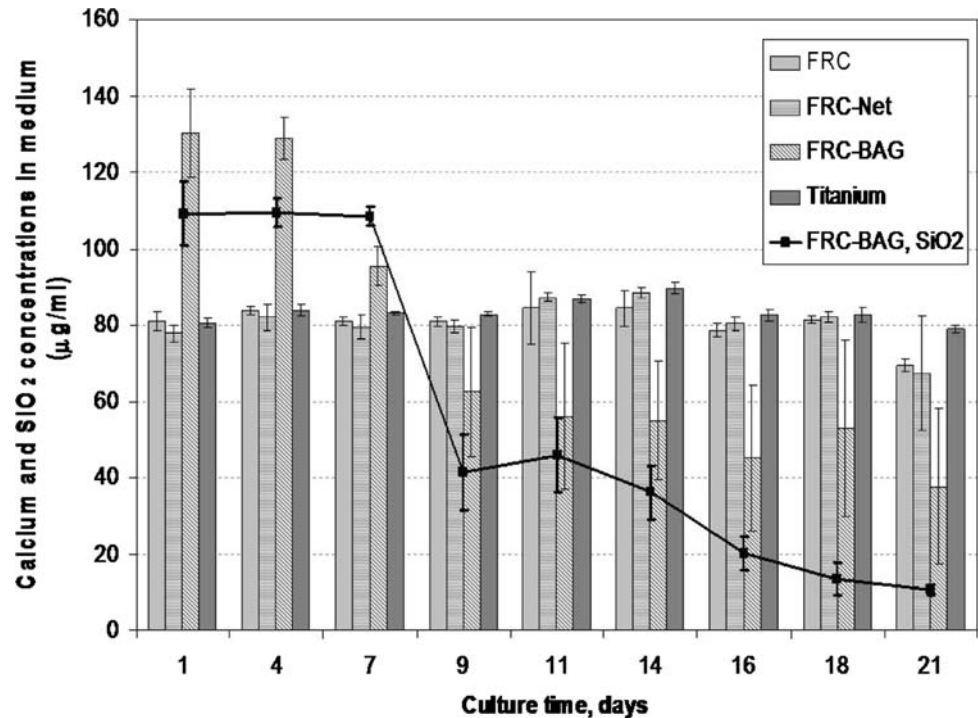
calcium precipitation on only four out of six analyzed FRC-BAG substrates. By day 14 calcium precipitation was observed with all the replicate specimens. Calcium depletion on FRC and FRC-Net did not take place until day 21 in culture. At that time precipitation was observed on all FRC, but only on half of the FRC-Net replicas. No calcium precipitation was observed on titanium substrates at any time.

### 3.5 Gene expression

The progress of osteogenic differentiation is summarized in Fig. 7. The gene expression profile of the cell stock used to seed the scaffolds indicated clear signs of osteogenicity ( $\Delta C_T$ , BSP = 1.85,  $\Delta C_T$ , OC = -4.15).

Strong, and statistically significant ( $P < 0.05$ ) induction of BSP was observed with all materials after 7 days in

**Fig. 6** Evolution of calcium (columns) and silica (line) concentrations in culture medium. The calcium level in fresh culture medium is ~80 µg/ml. Error bars represent standard deviations



culture. In contrast, clear OC induction did not take place until day 14, although FRC and FRC-Net showed a slight induction already at 7 days. No further changes in the gene expression levels were observed, except with titanium, in which case the BSP and OC expression at 21 days was significantly higher than at 7 days and 14 days, respectively.

The fastest osteogenic differentiation seemed to take place on FRC. Specifically, statistically significant differences after seven days were observed in OC expression when compared to titanium ( $P = 0.008$ ), and in both the BSP and OC expression levels when compared to FRC-BAG ( $P = 0.012$  and  $P = 0.011$ ). In contrast, a prolonged differentiation process was observed on titanium, with a higher OC expression level than on any other tested material ( $P < 0.015$ ) at 21 days. At that time, BSP expression on titanium also seemed to be increased compared to FRC-BAG ( $P = 0.058$ ) and to FRC-Net ( $P = 0.050$ ), although with ambiguous statistics. No other differences among the tested materials were observed.

#### 4 Discussion

Titanium and its alloys are considered to be biocompatible materials for bone contact applications. This has been largely attributed to the corrosion-resistant oxide layer forming on the implant surfaces [35]. In this study we have shown that osteoblast attachment, proliferation and differentiation on the BisGMA-TEGMA polymer with E-glass

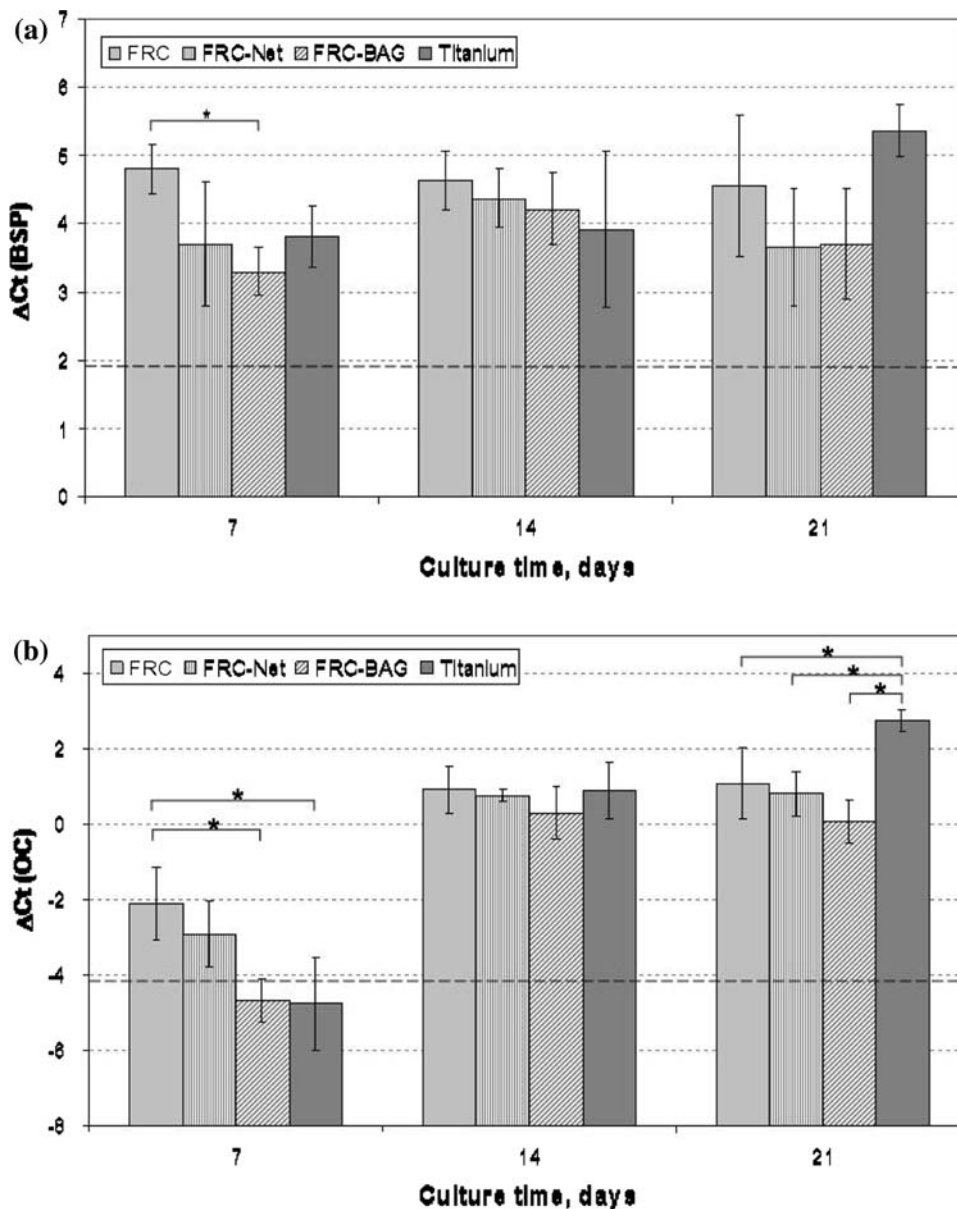
fiber reinforcement is comparable with that observed on titanium. An additional aim of the present study was to analyze the osteoblast response to FRC, with or without BAG coating. Furthermore, the effect of exposed E-glass fibers was evaluated.

The introduction of a new biomaterial for surgery requires a certain number of preclinical studies. The three different FRC substructures used in this study were made of pBis-GMA-pTEGDMA copolymer, which is already used clinically as approved bone cement [36–38]. All the tested specimens were blasted with similar sized aluminum oxide particles to produce comparable surface roughness on each material. Although, most of the surface roughness investigations have evaluated the osteoblast behavior on micro-structured surfaces [39], recent research emphasizes that in addition to the micro topography, cells use the nano topography of the substrate for orientation and migration [40, 41].

The blasting process also exposed some of the E-glass fibers on the FRC-Net, but this did not show any adverse effects on the cultured cells. Aluminum oxide particles were used for the blasting as it has been shown that the presence of alumina particles on blasted titanium does not interfere with bone apposition in in vivo conditions [42]. The higher final surface roughness of FRC specimens compared to titanium is due to the softness of the polymer surface, resulting in higher abrasion of the surfaces.

SEM observation showed that the cultured cells proliferated on all the blasted surfaces, and eventually formed multicellular layers entirely covering the specimens.

**Fig. 7** The progress of osteogenic differentiation, BSP (a), OC (b), during 3 weeks culture. The expression levels in the initial cell stock are marked with dashed lines. Error bars represent standard deviations and \* indicates a statistically significant difference ( $P < 0.05$ ) between materials



Within 21 days of culture no visible differences could be noted among different FRC substrates and titanium, indicating that the tested FRCs are cytocompatible materials with a cellular response similar to that on titanium.

Alkaline phosphatase activity, bone sialoprotein, osteocalcin production and mineralizing phenotype are important parameters typically used as markers of osteoblastic differentiation. The normal differentiation process includes a reciprocal relationship between proliferation and differentiation of osteogenic cells [43, 44]. Accordingly, the cells on FRC-BAG stopped expanding and their ALP activity reached peak value during the second week of culture. Furthermore, their gene expression profiles increased to levels similar to those on the other surfaces, and the cells started to mineralize more rapidly than the

cells seeded on the other materials. The enhanced differentiation cascade with FRC-BAG is probably related to Ca, PO<sub>4</sub>, and Si ions initially released from the BAG [24, 25]. The osteoblasts cultured on FRC-BAG showed a different trend in the calcium and silicon content of the culture medium compared with the other materials. The Ca and Si ions released from the bioactive glasses are known to stimulate the osteoblastic function and maturation [45].

Hench and West have proposed that the release of soluble silica from the surface of bioactive glasses might be at least partially responsible for stimulating the proliferation of bone-forming cells on bioactive glass surfaces [46]. However, the accumulating mineral phase inhibited further BAG dissolution, resulting in rapidly decreasing silica concentrations.



The results of this study support the initial working hypothesis that the addition of BAG particles promotes osteoblast behavior on FRC. However, the results achieved in static cell culture conditions cannot directly be extrapolated to clinical conditions.

## 5 Conclusion

The good biocompatibility of the experimental FRC substrates in a cell culture condition indicates that these materials have good potential to promote bone cell interactions and bone bonding. Furthermore, FRC with BAG coating showed enhanced osteogenic differentiation, which makes it probably the best candidate for further in vivo studies.

**Acknowledgments** The first author would like to thank the ITI foundation for a research scholarship. This work has been carried out within the Bio- and Nanopolymers Research Group of the Academy of Finland (CoE program 77317, Academy of Finland Grant No: 200077) and was partially funded by the Finnish National Technology Agency, TEKES (No: 40319/02).

## References

1. A.K. Roynesdal, E. Ambjornse, S. Stovne, H.R. Haanaes, *Int. J. Oral Maxillofac. Implants* **13**, 500 (1998)
2. J.A. Porter, J.A. Von Fraunhofer, *Gen. Dent.* **53**, 423 (2005)
3. Z. Schwartz, B.D. Boyan, *J. Cell Biochem.* **56**, 340 (1994)
4. K. Mustafa, A. Wennerberg, J. Wroblewski, K. Hultenby, B.S. Lopez, K. Arvidson, *Clin. Oral Implants Res.* **12**, 515 (2001)
5. M. Bächle, R.J. Kohal, *Clin. Oral Implants Res.* **15**, 683 (2004)
6. K. Kieswetter, Z. Schwartz, T.W. Hummert, D.L. Cochran, J. Simpson, D.D. Dean, B.D. Boyan, *J. Biomed. Mater. Res.* **32**, 55 (1996)
7. D. Buser, N. Broggini, M. Wieland, R.K. Schenk, A.J. Denzer, D.L. Cochran, B. Hoffmann, A. Lussi, S.G. Steinemann, *J. Dent.* **32**, 529 (2004)
8. K. Kurioka, M. Umeda, O. Teranobu, T. Komori, *Kobe J. Med. Sci.* **45**, 149 (1999)
9. E.J. Cheal, M. Spector, W.C. Hayes, *J. Orthop. Res.* **10**, 405 (1992)
10. A.J. Goldberg, C.J. Burstone, *Dent. Mater.* **8**, 197 (1992)
11. M.A. Freilich, J.P. Duncan, E.K. Alarcon, K.A. Eckrote, *J. Prosthet. Dent.* **88**, 449 (2002)
12. M. Berhr, M. Rosentritt, R. Lang, G. Handel, *Clin. Oral Implants Res.* **12**, 174 (2001)
13. J.P. Duncan, M.A. Freilich, C.J. Latvis, *J. Prosthet. Dent.* **84**, 200 (2000)
14. S.M. Tuusa, M.J. Peltola, T. Tirri, L.V. Lassila, P.K. Vallittu, *J. Biomed. Mater. Res. B Appl. Biomater.* **82**, 149 (2007)
15. A.J. Aho, M. Hautamaki, R. Mattila, P. Alander, N. Strandberg, J. Rekola, J. Gunn, L.V. Lassila, P.K. Vallittu, *Cell Tissue Bank.* **5**, 213 (2004)
16. A.M. Ballo, L.V. Lassila, P.K. Vallittu, T.O. Närhi, *J. Mater. Sci: Mater. Med.* **18**, 2025 (2007)
17. M. Svehla, P. Morberg, W. Bruce, W.R. Walsh, *J. Biomed. Mater. Res. B Appl. Biomater.* **74**, 423 (2005)
18. H. Gollwitzer, P. Thomas, P. Diehl, E. Steinhauser, B. Summer, S. Barnstorf, L. Gerdesmeyer, W. Mittelmeier, A. Stemberger, *J. Orthop. Res.* **23**, 802 (2005)
19. K. Soballe, K. Gotfredsen, H. Brockstedt-Rasmussen, P.T. Nielsen, K. Rechnagel, *Clin. Orthop.* **272**, 255 (1991)
20. S.H. Maxian, J.P. Zawadsky, M.G. Dunn, *J. Biomed. Mater. Res.* **27**, 717 (1993)
21. S.H. Maxian, J.P. Zawadsky, M.G. Dunn, *J. Biomed. Mater. Res.* **28**, 1311 (1994)
22. L.L. Hench, J. Wilson, *Science* **226**, 630 (1984)
23. Y. Fujishiro, L.L. Hench, H. Oonishi, *J. Mater. Sci. Mater. Med.* **8**, 649 (1997)
24. L.L. Hench, I.D. Xynos, J.M. Polak, *J. Biomater. Sci. Polym. Ed.* **15**, 543 (2004)
25. S. Radin, G. Reilly, G. Bhargave, P.S. Leboy, P. Ducheyne, *J. Biomed. Mater. Res. A* **73**, 21 (2005)
26. N. Price, S.P. Bendall, C. Frondoza, R.H. Jinnah, D.S. Hungerford, *J. Biomed. Mater. Res.* **37**, 394 (1997)
27. H.R. Stanley, L. Hench, R. Going, C. Bennett, S.J. Chellemi, C. King, N. Ingersoll, E. Ethridge, K. Kreutziger, *Oral Surg. Oral Med. Oral Pathol.* **42**, 339 (1976)
28. H.R. Stanley, L. Hench, R. Going, C. Bennett, S.J. Chellemi, C. King, N. Ingersoll, E. Ethridge, K. Kreutziger, *J. Oral Implantol.* **2**, 26 (1981)
29. N.N. Aldini, M. Fini, G. Giavaresi, *J. Biomed. Mater. Res.* **61**, 282 (2002)
30. N. Moritz, S. Rossi, E. Vedel, T. Tirri, H. Ylanen, H. Aro, T. Närhi, *J. Mater. Sci. Mater. Med.* **15**, 795 (2004)
31. C. Maniopoulos, J. Sodek, A.H. Melcher, *Cell Tissue Res.* **254**, 317 (1988)
32. K.A. Fanning, M.E.Q. Pilon, *Anal. Chem.* **45**, 136 (1973)
33. K. Lorentz, *Clin. Chim. Acta.* **126**, 327 (1982)
34. K.B. Jonsson, A. Frost, R. Larsson, S. Ljunghall, Ö. Ljunggren, *Calcif. Tissue Int.* **60**, 30 (1997)
35. R.T. Bothe, L.E. Beaton, H.A. Davenport, *Surg. Gynecol. Obstet.* **7**, 589 (1940)
36. S.L. Evans, C.M. Hunt, S. Ahuja, *J. Mater. Sci. Mater. Med.* **13**, 1143 (2002)
37. J. Palussiere, J. Berge, A. Gangi, A. Cotten, A. Pasco, R. Bertagnoli, H. Jaksche, P. Carpeggiani, H. Deramond, *Eur. Spine J.* **14**, 982 (2005)
38. G.S. Andreassen, P.R. Hoiness, I. Skraamm, O. Granlund, L. Engebretsen, *Arch. Orthop. Trauma Surg.* **124**, 161 (2004)
39. J.L. Ong, C.A. Hoppe, H.L. Cardenas, R. Cavin, D.L. Carnes, A. Sogal, G.N. Raikar, *J. Biomed. Mater. Res.* **39**, 176 (1998)
40. A.S.G. Curtis, C. Wilkinson, *Trends Biotechnol.* **19**, 97 (2001)
41. M.J. Dalby, L. Di Silvio, G.W. Davies, W. Bonfield, *J. Mater. Sci: Mater. Med.* **11**, 805 (2000)
42. A. Wennerberg, T. Albrektsson, C. Johansson, B. Andersson, *Biomaterials* **17**, 15 (1996)
43. G.S. Stein, J.B. Lian, T.A. Owen, *FASEB J.* **4**, 3111 (1990)
44. L. Malaval, D. Modrowski, A.K. Gupta, J.E. Aubin, *J. Cell. Physiol.* **158**, 555 (1994)
45. J. Yao, S. Radin, G. Reilly, P.S. Leboy, P. Ducheyne, *J. Biomed. Mater. Res. A* **75**, 794 (2005)
46. L.L. Hench, J.K. West, *Life Chemistry Reports* (Harwood Academic Publishers, Amsterdam, The Netherlands, 1996), p. 178